

Characterizing the Inter-Core Qubit Traffic in Large-Scale Quantum Modular Architectures

SAHAR BEN RACHED, Universitat Politècnica de Catalunya, Spain

ISAAC LOPEZ AGUDO, Universitat Politècnica de Catalunya, Spain

SANTIAGO RODRIGO, Universitat Politècnica de Catalunya, Spain

MEDINA BANDIC, Delft University of Technology, The Netherlands

SEBASTIAN FELD, Delft University of Technology, The Netherlands

HANS VAN SOMEREN, Delft University of Technology, The Netherlands

EDUARD ALARCÓN, Universitat Politècnica de Catalunya, Spain

CARMEN G. ALMUDÉVER, Universitat Politècnica de València, Spain

SERGI ABADAL, Universitat Politècnica de Catalunya, Spain

Modular quantum processor architectures are envisioned as a promising solution for the scalability of quantum computing systems beyond the Noisy Intermediate Scale Quantum (NISQ) devices era. Based upon interconnecting tens to hundreds of quantum cores via a quantum intranet, this approach unravels the pressing limitations of densely qubit-packed monolithic processors, mainly by mitigating the requirements of qubit control and enhancing qubit isolation, and therefore enables executing large-scale algorithms on quantum computers. In order to optimize such architectures, it is crucial to analyze the quantum state transfers occurring via inter-core communication networks, referred to as inter-core qubit traffic. This would also provide insights to improve the software and hardware stack for multi-core quantum computers. To this aim, we present a pioneering characterization of the spatio-temporal inter-core qubit traffic in large-scale circuits. The programs are executed on an all-to-all connected multi-core architecture that supports up to around 1000 qubits. We characterize the qubit traffic based on multiple performance metrics to assess the computational process and the communication overhead. Based on the showcased results, we conclude on the scalability of the presented algorithms, provide a set of guidelines to improve mapping quantum circuits to multi-core processors, and lay the foundations of benchmarking large-scale multi-core architectures.

CCS Concepts: • **Computer systems organization** → **Quantum computing**; • **Networks** → **Network performance analysis**.

Additional Key Words and Phrases: Modular Quantum Computers, Quantum Communications

1 INTRODUCTION

Quantum computing technology has witnessed a substantial progress in hardware development and software design over the past decade in pursuit of fault-tolerant quantum computers [42]. In principle, unlocking their long-awaited computational power is contingent on integrating thousands to millions of qubits into robust processors. Yet, densely-packed monolithic quantum processors raise several issues that deteriorate the computational results; mainly due to the effect of crosstalk, quantum state disturbance, and the increased complexity of the control system [45]. Building multi-core quantum processors has been introduced among the most promising strategies to scale the contemporary Noisy Intermediate Scale Quantum (NISQ) devices [44] considering the various types of

Authors' addresses: Sahar Ben Rached, Universitat Politècnica de Catalunya, Carrer de Jordi Girona, 31, Barcelona, Catalunya, Spain, 08034, sahar.benrached@upc.edu; Isaac Lopez Agudo, Universitat Politècnica de Catalunya, Carrer de Jordi Girona, 31, Barcelona, Catalunya, Spain, 08034, isaac.lopez@upc.edu; Santiago Rodrigo, Universitat Politècnica de Catalunya, Carrer de Jordi Girona, 31, Barcelona, Catalunya, Spain, 08034, srodrigo@ac.upc.edu; Medina Bandic, Delft University of Technology, Mekelweg 5, Delft, South Holland, The Netherlands, m.bandic@tudelft.nl; Sebastian Feld, Delft University of Technology, Mekelweg 5, Delft, South Holland, The Netherlands, s.feld@tudelft.nl; Hans van Someren, Delft University of Technology, Mekelweg 5, Delft, South Holland, The Netherlands, j.vansomeren-1@tudelft.nl; Eduard Alarcón, Universitat Politècnica de Catalunya, Carrer de Jordi Girona, 31, Barcelona, Catalunya, Spain, 08034, eduard.alarcon@upc.edu; Carmen G. Almudéver, Universitat Politècnica de València, Camí de Vera, s/n, València, València, Spain, cargara2@disca.upv.es; Sergi Abadal, Universitat Politècnica de Catalunya, Carrer de Jordi Girona, 31, Barcelona, Catalunya, Spain, 08034, abadal@ac.upc.edu.

processor technologies [13, 24, 30, 37, 47, 60, 60]. The main aim of this approach is addressing the aforementioned issues and scaling quantum processors to a size where complex problems could be practically solved.

The multi-core quantum approach is termed after the technique traditionally used in classical computing to enhance the performance of CPUs owing to multitasking [28], energy efficiency [34], on-demand hardware scalability, improved resource utilization, and parallel processing for specific tasks [16]. In classical multi-core computing, designing efficient Networks-on-Chip (NoCs) and inter-core networking is of significant importance as it directly impacts the overall processor performance. To setup a systematic network, it is critical to understand the traffic it serves. Consequently, substantial efforts have been dedicated to characterizing the communication occurring within multi-core systems and the adapted applications. Early research by Soteriou et al. [51] focused on analyzing a range of multiprocessors with 16 to 32 cores, using standard benchmark suites such as SPEC or PARSEC to explore temporal burstiness, spatial hotspotness, and source-destination distance. Barrow et al. [8] relied on the same methods to analyze the memory sharing patterns leading to certain traffic characteristics. Later studies extended the analyses to larger systems with up to 64 cores, examining specific aspects like time-varying traffic characteristics [11], in addition to the impact of specific architectural choices such as the cache coherence protocol on the communications [1, 2]. The workload characterization studies notably advanced the chip-scale networks field. Indeed, such contributions allowed researchers to analyze the correlation between particular traffic characteristics and on-chip network congestion [25], create synthetic traffic generators that better represented real workloads for NoC evaluation [1, 11, 51], and eventually guided the design of improved topologies, routing policies, and congestion control mechanisms at the chip scale.

In quantum computing, multi-core processors are designed by interconnecting smaller-sized cores with tens to hundreds of qubits via a chip-scale intranet that enables quantum state transfer between cores, as envisioned in Figure 1. This technique harnesses quantum parallelization while alleviating the qubit control requirements and enhancing the qubits isolation [45]. Therefore, modular architectures are envisioned to facilitate the integration of thousands to millions of qubits in a single system.

However, building multi-core processors still comes with its own set of challenges as quantum communications are highly latency-prone and impose additional technical inefficiencies to designing processors. Indeed, integrating chip-scale networks for quantum state transfer imposes a new paradigm as we need communication channels that maintain the quantum information and the properties of superposition and entanglement, rendering classical communication technologies impractical. Additionally, quantum state retransmission is not possible due to the fundamental limitation that forbids copying data due to the inherent qubit properties as stated by the no-cloning theorem [59]. Most critically, communication latencies induce a higher risk of data losses during the qubit transmission among cores due to state decoherence [46]. Several methods have been proposed to build inter-core communication networks for modular quantum computing architectures considering the aforementioned limitations and the diversity of technology platforms, such as integrating quantum links to interconnect superconducting chips [12], ion-shuttling for ion-trapped computers [31], photonic networks [37] and the teleportation protocol setup for state transfer [47]. Besides, the requirements for modularity extend beyond the qubit layer to impose further constraints at the networking, control, and compilation layers, hence the necessity of a consolidated software-hardware stack [21, 45].

As the early prototypes of quantum modular architectures are emerging, it is pertinent to employ analogous characterization techniques to classical computing while accounting for the fundamental differences between classical and quantum multiprocessors. Accordingly, a comprehensive analysis of the computational process and communication overhead in modular quantum processors would realistically represent the workloads and assess the performance of the system. Characterizing the performance of quantum computers has been advancing as the technology is developing, focusing mainly on benchmarking monolithic processors as will be detailed in Section 2.1. The work in [7] proposed methods for profiling quantum circuits based on their interaction graph parameters, aiming to improve compilation techniques. While the algorithms were executed on monolithic

processors hosting a limited number of qubits, this work gave insight into the circuit properties to consider for evaluating compilation algorithms and quantum processors. Early proposals for characterizing the spatio-temporal qubit traffic in modular architectures have recently been presented as well. Our prior work in [48] introduced a set of tools to extract and analyze the inter-core qubit traffic of quantum algorithms executed on multi-core processors of 128 qubits using the OpenQL compiler.

In this paper, we improve the methodology from our prior work by increasing the number of qubits, executing more application algorithms, introducing a set of performance metrics to assess the resources of the system, and analyzing the scalability of modular architectures in the strong and weak scaling. On this account, we present a pioneering inter-core qubit traffic analysis in multi-core architectures hosting around 1000 qubits by executing quantum algorithms of various structures. We interpret the inter-core qubit traffic as the qubit movement among cores orchestrated by the compiler to execute programs on modular architectures considering a given circuit mapping algorithm and particular communication techniques. We propose a custom set of performance metrics aiming to evaluate the required computation and communication resources for executing programs on modular processors. We conduct a thorough analysis of each circuit’s workload according to performance metrics of parallelization, resource usage uniformity, and spatio-temporal locality. We also assess the impact of the OpenQL circuit mapping algorithm and provide guidelines to improve compilation techniques for modular architectures. We designed our performance metrics based on current benchmarking techniques in quantum computing, and added metrics that specifically represent the inter-core communications.

This paper is organized as follows: in Section 2, we start by presenting the on-going research on methods for assessing quantum systems and developing compilation techniques for modular quantum computers. In Section 3, we propose our work methodology, the guidelines to define practical and scalable performance metrics for characterizing modular quantum processors, present our selected algorithms covering diverse applications, and introduce our set of performance metrics. The remainder of the paper showcases the results for circuit mapping and qubit traffic analysis in Section 4, followed by a thorough discussion in Section 5 on the impact of communication overhead on the overall computational process, the scalability of quantum algorithms in modular architectures, and designing adequate compilation techniques. We close with the main conclusions and future work in Section 6.

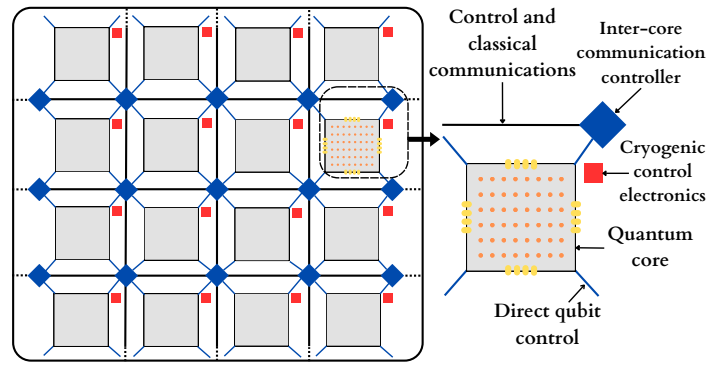


Fig. 1. Overview of the envisioned modular quantum computer architecture

2 RELATED WORK

2.1 Benchmarking quantum computers

Building modular quantum computers imposes new technology paradigms in manufacturing the Quantum Processing Units (QPUs), designing efficient compilers and developing near-term optimized applications. Benchmarking quantum processors has been evolving with the continuous progress of the field focusing solely on monolithic architectures. As the research efforts are pivoting towards multi-core processors, we propose performance metrics that may contribute to forming the early benchmarking suites for modular quantum processors. We consider several characteristics that continuously assess and measure the system's speed, efficiency, reliability, and identify areas for improvement and best practices.

Looking at the current state of benchmarking in quantum computing, we discern the various proposals covering the different layers of the system from the low-level qubit layer to high level applications, taking into account the diversity of qubit technologies:

- (1) **Physical benchmarking:** Considering the high risk of quantum state loss due to imperfect control and qubit interactions, evaluating the reliability of the computational processes in the presence of noise is necessary to determine the efficiency of a given device. Therefore, we refer to physical benchmarks that assemble a set of algorithms and models to understand the properties of a given quantum computer. There exists typical parameters that reflect the quality of the qubits and the overall performance of the control system, mainly the relaxation time T_1 , the dephasing time T_2 , single-qubit gate fidelity, two-qubit gate fidelity, and readout fidelity. These parameters are used in the quantum process tomography technique [41] to characterize the performance of any computation process, as well as the randomized benchmarking [33], which is an experimental method for measuring the average error rates of quantum computers by implementing long sequences of randomly sampled quantum gate operations. However, both of these methods scale poorly with the number of qubits and are only effective to evaluate processors with a small number of qubits. While physical benchmarks represent the properties of the device and are essential to detect points of improvement, they overlook the performance of the processor in solving algorithms and executing circuits.
- (2) **Synthetic benchmarking:** The efficiency of quantum computers is dependent on the performance of the system in executing circuits, especially for prototype devices. There are currently standard benchmarks for evaluating the NISQ devices' computational performance, such as the Quantum Volume [14] which is a single metric that considers several parameters, for instance gate fidelity and qubit coherence, to measure the largest square random quantum circuit that a quantum computer can execute reliably. The CLOPS [56] benchmark evaluates the speed, Quantum Volume quality, and scalability of the number of qubits. Yet, the reliance of these two metrics on randomness and the physical properties of the system limits their significance and scalability. A similar assessment we find particularly for ion-trapped computers is the Algorithmic Qubits [52]. It uses quantum algorithms rather than random circuits to determine the largest number of effectively perfect qubits that can be used for a program, considering error-correction and the qubit count. The quantum LINPACK benchmark [17] is developed to measure the performance of the quantum computer by its capacity to solve random systems of linear equations with dense random matrices, which may not capture the ability of the device to solve various applications.
- (3) **Application-oriented benchmarking:** Application-level benchmarks rely on the program results accuracy as an indicator of the quantum computer's computational capabilities and scalability. Due to the diversity of applications and their purposeful usage, this metric stands as a fundamental aspect for designing several widely-used benchmarking sets. The majority of these benchmarks use Variational Quantum Circuits (VQCs) to evaluate certain properties of the system, such as QPack [38] that implements the Max-Cut, dominating set, and Travelling Salesman Problem (TSP) circuits to capture the runtime,

best approximation error, success probability, and scalability. Additionally, QASMBench [35] is a cross-platform suite that executes quantum circuits of different problems to determine various circuit properties. SupermarQ [55] is also a benchmarking suite that includes diverse applications and evaluates real quantum devices of different platforms according to a customized set of performance metrics. Application-based benchmarks especially emphasize on the practical use of algorithms to estimate the different parameters and properties of quantum computers, despite the divergence of their performance metrics and targeted analysis.

The aforementioned benchmarks are applicable exclusively for monolithic QPUs. For our work, they are useful in perceiving metrics that assess the performance of the system. We extend the current performance assessment metrics to include inter-core communication cost and overhead, not merely computation resources.

2.2 Compilation techniques for modular architectures

Compilers play a critical role in the quantum computing stack as they translate high-level quantum programming languages into executable instructions on qubits and apply the necessary modifications to the input circuit in order to meet the underlying hardware constraints. Due to the fundamental differences between quantum and classical computation, quantum compilers are designed to comply with the circuit-based quantum algorithm implementation and the problem size, and to account for the hardware technology properties, mainly qubit control and readout techniques and the processor topology.

Quantum compilers typically support specific programming languages which provide an abstract representation of the circuit gates, such as Qiskit [4], Cirq [3], Q# [39], among others. Compilers are mainly responsible of decomposing the input operations to native gates supported by the hardware device. In the process of translating operations to their low-level representations, compilers apply gate optimization techniques aiming to improve the efficiency and performance of quantum circuits. Quantum circuit mapping is also an important aspect of compilers, especially that contemporary hardware architectures often have limited connectivity between qubits. This aims to rearrange the connectivity of the system and qubit placement to allow the direct application of native two-qubit gates - mainly CNOT gates. Initial placement is usually employed to map virtual qubits from the high-level program to physical qubits on the device, taking into account the underlying connectivity constraints. Additionally, compilers handle qubit routing and scheduling for executing the gate operations optimally. For future fault-tolerant quantum computers, compilation techniques will include quantum error correction and fault tolerant protocols to reduce the impact of errors and improve the overall reliability of quantum computations.

Designing compilers for multi-core architectures specifically takes into account the inter-core operations necessary to apply two-qubit gates on qubits initially placed in different cores, for example by applying remote two-qubit gates [23] or inter-core quantum state transfer to bring interacting qubits into proximity [47]. Compilation algorithms for multi-core processors are coming into play to accommodate the various architectural constraints and communication requirements as the technology is developing. Several methods are under investigation, such as quantum circuit cutting and reconstruction [53], QUBO-formulated circuit mapping optimization approach [6], and qubit-to-core assignment considering the interactions between qubits over the circuit based on the Hungarian algorithm [20].

The communication resources should be characterized and optimized at the compilation level, since the inter-core communication technique determines the overhead and directly impacts the computational process. Furthermore, the qubit resource allocation, referring to the dedicated computation and communication qubits, poses further constraints on the computational resources and should be represented at the compiler level. Indeed, allocating more qubits for communication would allow a higher number of simultaneous inter-core communications. However, this would limit the number of computation qubits and therefore reduces necessary

computational resources. Hence, it is required to reach a trade-off of computation and communication qubits for designing algorithms and optimized compilation techniques for multi-core quantum computers.

3 METHODOLOGY

3.1 Work methodology

The primary goal of this study is to analyze the inter-core qubit traffic in modular quantum processors to assess their scalability. To achieve this, we follow the methodology depicted in the Figure 2. We compile different quantum circuits on various architecture sizes to generate inter-core communication traces. These traces are then analyzed to extract relevant data that formulate our performance metrics, which are further processed and graphically visualized.

For our work, we use OpenQL [32] to compile and optimize quantum circuits. The inter-core state transfer protocol applied is the teleportation-swap. This consists of applying two simultaneous teleportation operations in opposite directions between two cores to move a computation qubit into proximity with a second qubit in a different core and enabling two-qubit gate application. We consider a device architecture supporting an intra- and inter-core all-to-all connectivity. In this case, optimal initial placement and qubit routing are not needed, and the compiler initially maps virtual qubits directly to physical qubits. We also assume any idling qubit which state is not used for computation operations can be utilized as a communication qubit, and therefore favoring simultaneous application of inter-core communication operations. The mapping algorithm used by OpenQL is proposed by Baker et al. in [5]. This approach maps quantum algorithms on multi-core architectures by leveraging graph partitioning methods for the purpose of placing qubits in different chips with a minimum inter-core qubit movements.

In an analogy to the scalability analysis of classical multi-core computers, we implement circuits on modular architectures in two scaling regimes:

- **Strong scaling:** we fix the number of qubits per core and increase the number of cores. We analyze the performance of the system in the strong scaling to evaluate the communication overhead as we add more cores, and its impact on the computation process. We fix the size of a single core to 16 qubits, aiming to increase the number of cores and the size of circuits until around 1000 qubits. However, due to the high computational cost of certain algorithms and the current limitations of the compiler, it was not possible to execute all circuits at this size.
- **Weak scaling:** we keep the same problem size, i.e total number of qubits, and increase the number of cores. We inspect the performance of the system in the weak scaling aiming to assess how the program performance varies with the number of cores for a fixed problem size. In this case, the number of qubits per core varies, yet the total number of qubits is counting 512. However, due to the high computational cost of certain programs and the current limitations of the compiler, it was not possible to execute all circuits at a size of 512 qubits in this case as well.

We present the results of each circuit up to the largest size we could successfully implement.

3.2 System characterization design

For the purpose of analyzing the inter-core qubit traffic and determining the communication overhead, we evaluate the execution performance according to a customized set of metrics that considers both computation and communication resources as explained in Section 3.4.

We base our selection of applications upon five primary design guidelines:

- **Diversity of circuit structure:** different algorithms have different requirements and resources for an optimal execution on a modular architecture. Based on our analysis, we aim to correlate the algorithm

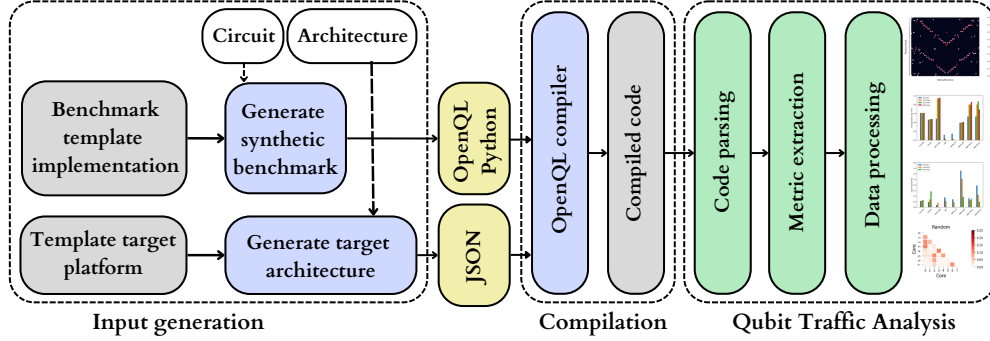


Fig. 2. Flow diagram of the qubit traffic analysis software tool

structure to the resource requirements. We therefore select a wide range of circuits, from structured to random algorithms, in order to analyze their operational constraints and communication overhead.

- **Application-oriented:** The multi-core processors approach aims to scale quantum computers to the size where they support large-scale real-world applications. We therefore select state-of-the-art sub-routines and algorithms envisioned to solve complex problems in physics [36], chemistry [43], finance [58], machine learning [10], and database search [27], among others.
- **Scalability:** The standard benchmarking techniques and performance metrics, such as Quantum Volume and randomized benchmarking, are not adequate to probe large-scale modular devices as their performance becomes intractable with the increasing number of qubits. Therefore, we implement circuits which sizes steadily increase with the number of qubits and can be executed on the envisioned large-scale quantum computers within the limits of current compilers.
- **Parallelization:** Parallelization is a key feature of executing algorithms on multi-core architectures that refers to the ability of running a program on multiple processors simultaneously by leveraging the inter-core communication network. If an algorithm is parallelizable, it can be optimally distributed on the architecture and takes advantages of the infrastructure to implement concurrent operations. On the other hand, if an algorithm is not easily parallelizable, it may not benefit from the multi-core architecture, or worse, the communication overhead deteriorates its performance.
- **Inter-core communication density:** Inter-core communication is the key component of modular architectures. In order to analyze the impact of communication networks and protocols on the computational process, we need algorithms with a high density of two-qubit gates and qubit operations applied across cores. We analyze the communication overhead originating from the inter-core state exchange.

3.3 Selected benchmarks

Quantum algorithms are better suited for evaluating the overall performance of the system, from the software to the hardware stack, than circuit or gate-based methods which rather assess the hardware performance. Therefore, including algorithms for potential applications is necessary to evaluate multi-core architectures. The selected circuits will be useful for a wide range of applications and domains where quantum computing is expected to be advantageous. The following algorithms are selected based on the previously defined criteria in 3.2.

We summarize the structure of each circuit implemented in Table 1, showcasing the two-qubit interconnectivity, i.e how the two-qubit gates are applied in the circuit, and the estimated gate count, referring to the upper bound on the number of gates. Further details on the gate count estimation is found in the Appendix A. We inspect

Table 1. Circuit structures of the implemented applications. N , q , k , and l indicate the total number of qubits, qubit index, number of iterations in the Grover’s circuit, and number of ansatz layers, respectively. The exact gate count depends on the circuit implementation, which may involve additional gates for initialization, measurement, and optimization techniques introduced by the compiler.

Circuit	Two-qubit interconnectivity	Estimated gate count
Cuccaro Adder	Nearest-neighbor	$\approx O(N)$
Grover	$\frac{N}{2}$ to $(\frac{N}{2} + 1)$ qubits	$\approx O(k \times N)$
GHZ State	One qubit to all	$\approx O(N)$
QFT	$(N - q)$ qubits to one	$\approx O(N^2)$
QAOA MaxCut Ansatz	Nearest-neighbor	$\approx O(l \times N)$
VQE HEA_1 and HEA_2	Nearest-neighbor	$\approx O(l \times N)$

the circuit structure to analyze the evolution of computation and communication resources as we increase the program size.

3.3.1 Cuccaro adder. The Cuccaro adder is an arithmetic operator designed for adding binary numbers of equal bit-string size using quantum computers [15]. The algorithm is based on the ripple-carry approach built using one ancilla qubit and by applying sequentially dependent CNOT and CCNOT gates, forming the Majority (MAJ) gate that computes the majority of three bits in place and the “UnMajority and Add” (UMA) gate. The circuit showcases a linear depth that favors its scalability, and we consider the algorithm’s ladder of controlled gates a useful pattern for characterizing the inter-core communication workload.

3.3.2 Grover’s main routine. Grover’s algorithm for solving unstructured database search problems is among the first developed quantum algorithms that demonstrates a quadratic speedup compared to its classical counterparts, which makes it a useful subroutine for multiple applications, for instance, power and energy applications [29] and quantum machine learning [18]. In essence, the algorithm applies amplitude amplification to increase the probability of measuring the correct answer at the end of the circuit. The main steps of the algorithm are state preparation, the oracle implementation to mark the correct answer depending on the problem input, and the diffusion operator that magnifies the probability of the correct answer before measurement. We implement the Grover’s main routine that starts by initializing the qubit to superposition states and applies iterative instructions to mark the correct answer and amplifies its state amplitude, also referred to as the oracle-diffuser cycle.

3.3.3 GHZ state. Entanglement is a key property to unlock the computational power of quantum processors. It is then important to evaluate the modular architecture’s support for large entangled states considering the long-range interactions and inter-core communication requirements. The Greenberger-Horne-Zeilinger state, known as the GHZ state [26], is a circuit-size maximally entangled state generated by applying the Hadamard gate on one qubit followed by a ladder of CNOT gates controlled by the qubit in superposition and targeting each of the remaining ones, producing the state

$$\frac{|00\dots 0\rangle + |11\dots 1\rangle}{\sqrt{2}}$$

We opted for the circuit implementation where the first qubit is set as the controller since the dependent ladder of CNOT gates serves our interest in monitoring long-range inter-core communications and qubit operations across cores.

3.3.4 Quantum Fourier Transform. The quantum Fourier Transform (QFT) [40] is a quantum computing routine that applies a discrete Fourier transform to the amplitudes of a wavefunction. It is a fundamental step in several quantum algorithms, including Shor’s factoring algorithm [50] and the quantum phase estimation [40]. It is implemented utilizing the Hadamard gate, phase shift gates, and controlled phase shift gates. The QFT is proven to be useful for several quantum applications that require large-scale architectures as well, mainly factoring large numbers and solving discrete logarithm problems, which have significant implications in advancing cryptography and computational complexity theory.

3.3.5 The Quantum Approximate Optimization Algorithm. The Quantum Approximate Optimization Algorithm (QAOA) [22] is a near-term hybrid algorithm designed for solving combinatorial optimization problems. The circuit input state is encoded as a graph where qubits represent the vertices of the graph. By formulating the optimization problem as a mathematical objective function to be minimized or maximized, the algorithm constructs a parameterized quantum circuit where the number of layers l is a tunable parameter and iteratively updates the circuit parameters based on the measured results using classical optimization approaches, aiming to improve the objective function. The best candidate solution is obtained by the end of a fixed number of iterations or until convergence is reached. For our work, we implemented the quantum circuit construction step that performs state preparations and measurements to solve the MaxCut problem of two randomly generated graphs: the Watts Strogatz graph which exhibits short, average path lengths and high clustering [57], and the Erdos Renyi graph [19] of edge probability 0.2. The number of vertices corresponds to the total number of qubits. We mainly focus on the circuit mapping and compilation on multi-core quantum devices, rather than solving the given problem. We utilize a circuit ansatz consisting of a sequence of single-qubit rotations and entangling CNOT gates.

3.3.6 The Variational Quantum Eigensolver. The Variational Quantum Eigensolver (VQE) is a hybrid chemistry algorithm designed to determine the ground state energy of a given Hamiltonian [43]. The VQE uses a classical optimization algorithm in combination with a parameterized quantum circuit to find the lowest eigenvalue, representing the ground state energy, and its corresponding eigenvector, representing the ground state, of a quantum system Hamiltonian, for example a molecule. The algorithm starts by selecting a parameterized circuit that defines a prepared variational state where the number of layers l is a tunable parameter, known as the ansatz. The choice of the ansatz is detrimental to the performance and accuracy of the algorithm. The following step consists of determining the Hamiltonian expectation value by performing measurements on the quantum state obtained from the previous step. Multiple measurements are required to estimate the expectation value accurately. Using a classical optimization algorithm, the parameters of the variational circuit are updated iteratively until the expectation value of the Hamiltonian is minimized. The solution is obtained when a convergence criterion is met, for instance when the expectation value reaches a certain threshold or the parameters converge to a stable value. At this stage, the parameters yielding the minimum expectation value are used to prepare the quantum state that represents the ground state of the Hamiltonian. For our work, we implement two different types of Hardware-efficient ansätze, the first displaying a sequential ladder of CNOT gates as depicted in [54], and the second showcasing parallel execution of CNOT gates as shown in [9]. We only focus on the compilation and mapping of the circuit on a multi-core architecture, and not solving a given problem.

3.4 Performance metrics for multi-core quantum processors

We evaluate the computational capacity of multi-core processors for executing our selected set of circuits according to several metrics that represent the computational performance and communication requirements. The introduced metrics characterize the communication overhead in modular architectures, the compilation process and potentially the technology of the processor.

3.4.1 Parallelization.

(1) Computation-to-Communication Ratio (CCR)

Circuit parallelization is advantageous for reducing the overall execution time by overlapping the operations and maximizing the utilization of resources. Executing quantum circuits on modular architectures demands implementing additional inter-core operations according to a given communication protocol, which presumably delays the computational tasks. Designing robust processors that achieve parallelization and an efficient computation process requires a trade-off for allocating computation and communication qubits. The inter-core communication protocol we employ for mapping circuits on modular architectures is the teleportation protocol as presented in [49]. We analyze the circuit parallelization by defining the computation-to-communication ratio (CCR) as the normalized ratio of average single- and two-qubit operations n_{ops} to the average number of teleportation operations n_{telep} per qubit:

$$CCR = \frac{n_{ops} - n_{telep}}{n_{ops} + n_{telep}} \quad (1)$$

If the ratio tends to 1, we conclude that computation tasks are dominating the execution process. If it tends to -1 then communications are dominating, and if it tends to 0 then the given architecture design meets the communication-to-computation trade-off.

3.4.2 Resource usage uniformity in space and time.

(1) Mean qubit hotspotness

Qubits are the key component in computations and inter-core communications as they store and manipulate quantum information. As the circuit size increases to host thousands of qubits and operate millions of gates, the relatively short qubit coherence time remains a significant challenge in the path to fault-tolerant computers. Mapping virtual circuits to physical qubits yields additional operations applied on qubits to comply with the compilation constraints. We investigate the qubit hotspotness in our analysis, which is related to the number of gates applied on physical qubits, to estimate the distribution uniformity of operations per qubit throughout the system. We account for both computation and teleportation operations. We define the mean qubit hotspotness as the ratio of the variance of operations applied to a physical qubit $\sigma_{ops/qubit}^2$ to the average operations applied to a physical qubit $\mu_{ops/qubit}$ following the compilation process:

$$\overline{H}_{qubit} = \frac{\sigma_{ops/qubit}^2}{\mu_{ops/qubit}} \quad (2)$$

(2) Mean core hotspotness

For an optimal usage of resources of the processor, the computation and communication operations need to be uniformly distributed across the cores as per the circuit requirements. We look into the core hotspotness during the program execution to identify the cores that operate inter-core communications and are mostly involved in the computation process. We correlate the core hotspotness to the distribution of inter-core communications in the system and define the mean core hotspotness as the ratio of the variance of teleportation operations $\sigma_{telep/core}^2$ to the average teleportation operations $\mu_{telep/core}$ for every core:

$$\overline{H}_{core} = \frac{\sigma_{telep/core}^2}{\mu_{telep/core}} \quad (3)$$

(3) Longest gate sequence

Since qubits are highly susceptible to state disruptions mainly due to gate application, performing a long sequence of gates would presumably result in deteriorating the computational process. As we scale the

circuit size, we look into the increment of operations executed. For our analysis, we determine the longest gate sequence as the maximum number of gates applied to any virtual qubit in a given circuit:

$$G = \max_{\forall q} |G_{ij}| \quad (4)$$

where G_{ij} is the set of gates operating qubits i and j .

Estimating the number of operations needed to execute a given circuit provides insight into the capacity of quantum devices to support large-scale computations within the limits of the qubit technology.

(4) Qubit lifespan

An additional metric that characterizes the capacity of the system to execute large-scale circuits within the limits of qubit technology and decoherence times is the qubit lifespan. We interpret the qubit lifespan as the maximum timeslice length that separates the first and the last gate applied to a physical qubit in a given circuit over the execution timeslices:

$$L = \max_q L_q \quad (5)$$

where

$$L_q = \max_{q \in \{i,j\}} T_{exec}(G_{ij}) - \min_{q \in \{i,j\}} T_{exec}(G_{ij})$$

such that $T_{exec}(g)$ corresponds to the execution timeslice of a specific gate g .

(5) Temporal burstiness

We look into the inter-core communication burstiness throughout the program execution for the purpose of monitoring the teleportation clustering in timeslices. The system is supposed bursty if there exists timeslices exhibiting a high number of teleportation operations clustered subsequently, followed by timeslices of low or spaced inter-core communications. This implies a non-uniform distribution of communications over runtime and directly impacts the performance of the system, resource allocation, and operation scheduling. Accordingly, it is crucial to investigate methods indicating the bursty behavior in order to distribute resources more evenly, and improve the overall system performance and stability. We characterize the burstiness of a quantum system as the ratio of the variance of parallel teleportations $\sigma_{telep(t)}^2$ to the mean of parallel teleportations throughout the execution timeslices $\mu_{telep(t)}$:

$$\bar{B} = \frac{\sigma_{telep(t)}^2}{\mu_{telep(t)}} \quad (6)$$

3.4.3 Locality. Mapping circuits to modular architectures requires specific compilation techniques that include intra-core qubit swapping and communication protocols that rely on inter-core qubit mobility for state transfer. It is then crucial to characterize the qubits' spatial and temporal locality for the purpose of evaluating the circuit partitioning techniques employed at the compiler level.

(1) Qubit temporal locality

We estimate the qubit temporal locality by the required number of teleportation operations. This describes the circuit partitioning uniformity as the communication requirements are evolving, and designates the optimal architecture components, i.e. are the number of cores and the number of qubits per core, that ensure the maximum stability and resource uniformity. We quantify the qubit temporal locality as the total amount of teleportation required for a given circuit execution:

$$T = \sum_{ts} T_{ts} \quad (7)$$

where T_{ts} is the number of teleportation per timeslice.

(2) Qubit spatial locality

The qubit spatial locality refers to the average duration that a logical qubit stays in a specific core, indicating the frequency of inter-core qubit movements. A higher average stay-time implies qubits remain relatively stationary, thus minimizing disturbance of their states. However, a lower average stay-time indicates frequent movement of qubits, which increases the risk of state loss. Therefore, maintaining a longer average stay-time is desirable to preserve the qubits' stability and minimize the risk of data losses. We define the qubit spatial locality as the average of qubit stay-time in a core over the program execution time:

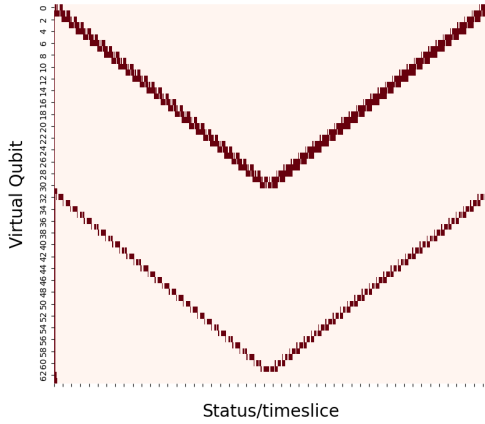
$$S = \frac{d_{qubit/core}}{t_{exec}} \quad (8)$$

where $d_{qubit/core}$ is the average stay-time of a qubit in a core and the t_{exec} is the total execution time defined in timeslices.

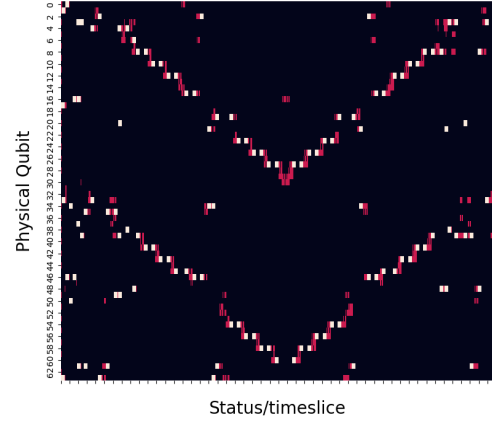
4 RESULTS

4.1 Impact of circuit mapping

The virtual mapping reflects the structure of the input circuit regardless of the underlying architecture, as it is shown for the Cuccaro Adder circuit in Figure 3a. The virtual mapping trace conveys the distribution of computation qubits and times. On the other hand, the physical mapping trace in Figure 3b showcasing the Cuccaro Adder circuit mapping to physical qubits on a modular architecture displays the computation, communication and idling qubits and times. This presents a general overview of the necessary resources to be allocated for a program execution considering a given architecture.



(a) The Cuccaro Adder circuit mapping to virtual qubits on an architecture of 64 qubits. Computation times are represented in red



(b) The Cuccaro Adder circuit mapping to physical qubits on a modular architecture of 16 qubits \times 4 cores with all-to-all connectivity. Computation, communication, and idling times are represented in red, white, and black, respectively

Fig. 3. The Cuccaro Adder circuit mapping to virtual and physical qubits

Circuit mapping on the physical architecture as performed by the compiler imposes several changes to the circuit structure. These structural changes exhibit the application of the mapping algorithm which aims to move qubits across processors in order to place interacting qubits into adjacent positions. The teleportation protocol is

applied if two interacting qubits are initially placed in different cores. Correspondingly, allocating more qubits into a single core would reduce the amount of teleportations required as local qubit interaction are favoured. While this setup would mitigate the communication overhead, it results in imposing the architectural constraints originating from a densely-packed quantum processor, as introduced beforehand. We present the circuit mapping traces of the various executed circuits in Appendix B. Additionally, we state that the circuit structure and qubit interactions are essentially algorithm dependent. The QAOA_02 and QAOA_WS circuits, for instance, implement the same ansatz yet different input graphs. Consequently, the corresponding virtual mapping traces are entirely different, indicating distinct circuit structures. This also impacts the number of gates applied and the inter-core operations required.

Circuits characterized with short-range intra- and inter-core gates where two-qubit operations are applied on nearest-neighbor or local qubits, such as Cuccaro, Grover, and QAOA_WS, tend to preserve their structures after the mapping process, meaning not many qubit movements were required to comply with an optimal mapping to physical qubits. The given architecture and the circuit partitioning algorithm are then advantageous for the execution of these circuits, as the topology is compatible with the circuit structures. For algorithms that require long-range two-qubit gates, and extensive parallel execution of two qubit gates, such as for GHZ, QFT, QAOA_02 and VQE HEA_1, the compiler imposes several rearrangement of qubit placements to comply with the input instructions. Since these circuits are characterized by a high density of two-qubit gates applied in parallel and interacting qubits placed in different cores, we note scattered communication and computation operations in their corresponding physical circuits. The GHZ circuit is a particular example of sequential two-qubit gates applied from one qubit to all others, and therefore exhibits both local, short-range and cross-core, long-range operations, which require extensive inter-core qubit movement. In the physical mapping, we show that the compiler moves the target qubits to the first core where the qubit 0 is located to enable the direct application of CNOTs. This appoints a frequent qubit movement and serial application of teleportation instructions. Generally, the larger the number of cores, the more inter-core operations are required, especially if the number of qubits per core is limited relatively to the circuit size. The mapping process gets more complex with a large number of cores, particularly for circuits exhibiting a high number of gates such as the QFT and QAOA_02 instances. This presumably gives an explanation for the scattered operation patterns and noticeable transformations from virtual to physical mapping.

4.2 Strong scaling

We analyze the performance of the system in the strong scaling to evaluate the communication overhead as we add more cores, and its impact on the computation process. We fixed the size of a single core to 16 qubits. We aimed to increase the number of cores and the size of circuits until 1000 qubits. However, due to the high computational cost of certain algorithms and the current limitations of the compiler, it was not possible to execute all circuits at this size. We present the results of each circuit up to the largest size we could successfully implement.

The first metric we interpret is the distribution of computation and communication operations over the execution time-slices as an indicator of an optimized workload. In principle, communication tasks take longer times than computation operations. Looking at the results in Figure 4 showcasing the distribution of required computational and communication temporal resources over the execution timeslices, we conclude that the circuit structure is a deterministic factor in parallelizing the operations.

Structured circuits that implement sequential two-qubit gates applied on adjacent or local qubits, mainly the Cuccaro and Grover's, indicate that the computation operations are not delayed by the communications despite the increasing number of qubits and operations. The system achieves an optimal rate of parallelizing computation and communication instructions as we increase the number of cores.

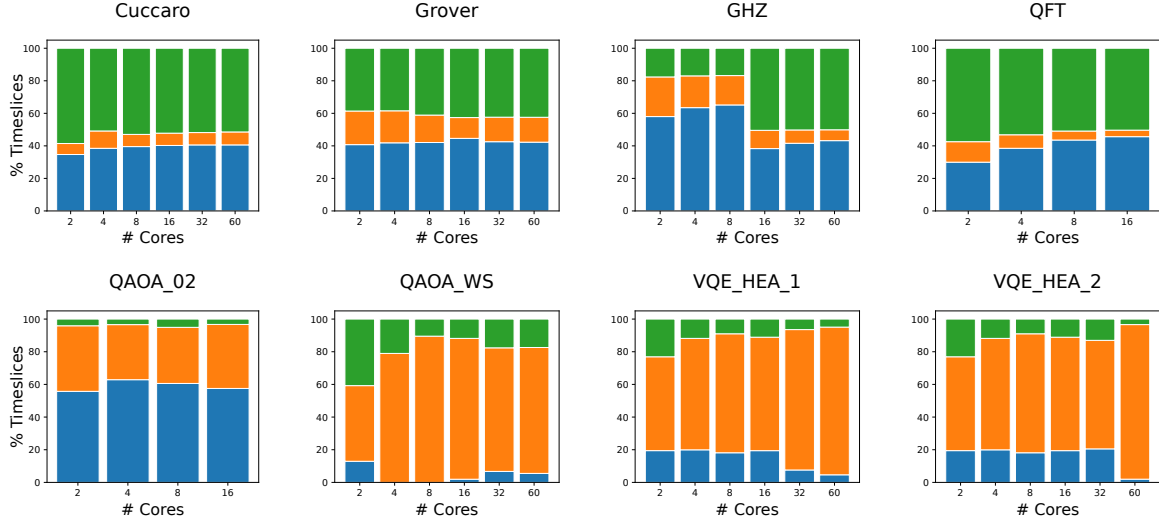


Fig. 4. Distribution of computation and communication operations over the execution timeslices in the strong scaling. Blue, orange, and green indicate the communication, parallel communication and computation, and computation operations, respectively.

The GHZ circuit exhibits a sequential application of CNOT gates as well. However, since the first qubit is in constant interaction with the rest of the qubits, adding cores results in increasing the likelihood of two-qubit gates applied across cores. The inter-core communications continuously increase at a high cost, hindering the computational operations. Yet, the compiler starts to improve the operation parallelization process as we scale to 16 cores. Looking at the compilation process output, we find that a reduction in the 8-core circuit execution duration induced this change of pattern. As the size of QFT circuit increases, the inter-core communication requirements grow without blocking the computational process. The QAOA_02 circuit is characterized by random gate application as imposed by the input graph, which explains the scattered pattern of communication and computational tasks, resulting in prohibitive communication execution times. The circuit size of QFT and QAOA_02 algorithms become too computationally costly over 16 cores, as the number of gates surges beyond the capacity of the compiler. The QAOA_WS circuit displays a favourable rate of operation increase, owing to sequential execution of CNOT gates. The VQE_HEA_1 and VQE_HEA_2 circuits showcase a similar pattern to QAOA_WS, where the first is characterized by a high number of subsequently-dependent CNOT gates applied to consecutive qubits, and the second displays an extensive parallel application of operations. Essentially, monitoring the temporal resources needed for inter-core communication is crucial, as the communication overhead translates to a higher risk of quantum state loss, and hence deteriorating the computational results.

We analyze the computation and communication process according to a set of metrics as depicted in Figure 5.

Circuits differ in the number of gates and the distribution of two-qubit operations. Overall, these differences are reflected in the varying resource requirements. The computation-to-communication rate tends to 1 for all circuits at different architecture sizes, indicating the computation operations are dominating the execution process, and therefore significant qubit resources are allocated to the computational tasks. The mean core hotspotness tends to increase as we scale the algorithm size for all types of circuits, showcasing the number of cores involved in the communication process. The longest gate sequence and the qubit lifespan increase as we scale the circuit

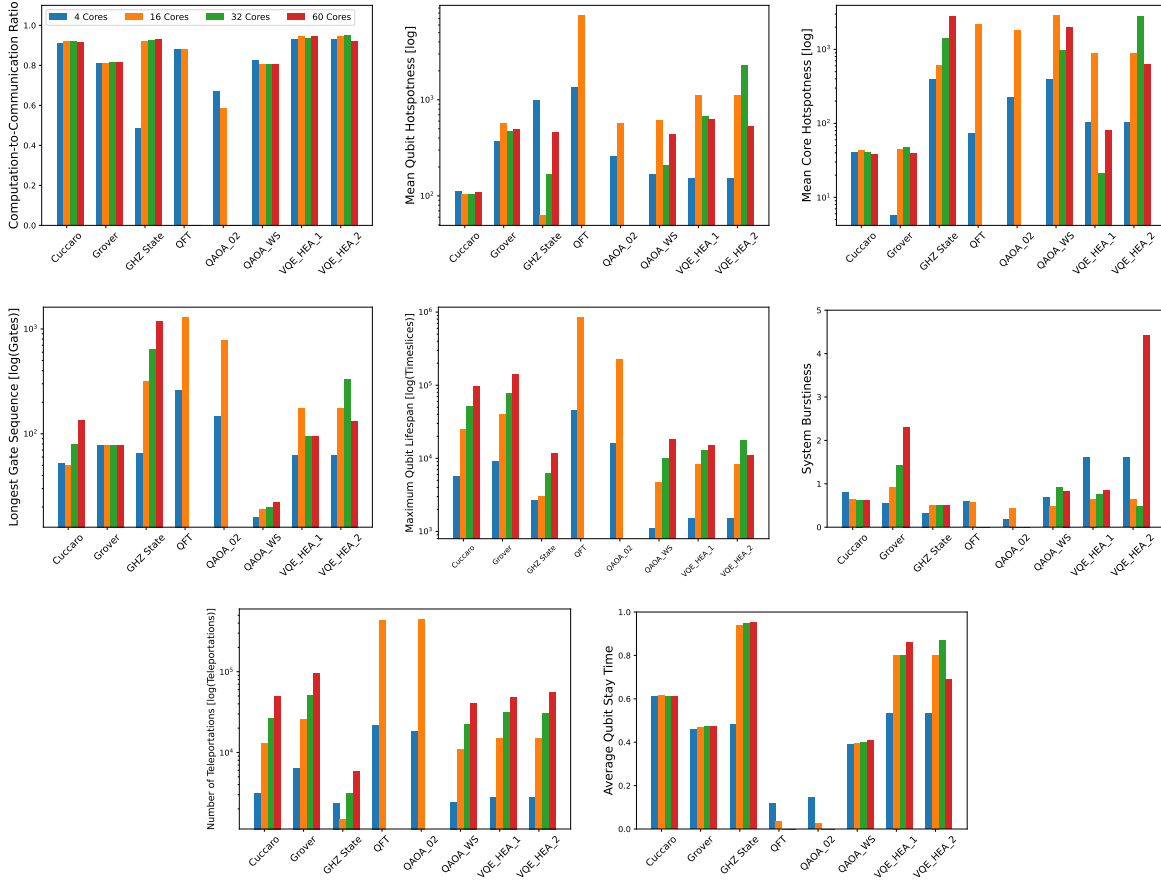


Fig. 5. Performance metrics for the selected algorithms executed on large-scale modular architectures supporting around 1000 qubits in the strong scaling

since the circuit depth is expected to increase, especially for circuits with a high density of two-qubit gates, mainly QFT. As for the GHZ state circuit, the longest gate sequence refers to the interaction of the first qubit with the remaining qubits, which surges as we increase the program size. However, despite a high number of operations applied, the execution time of this circuit is relatively shorter and therefore, we note a short qubit lifespan. We denote a relatively low communication burstiness for all circuits, which reveals the compilation process is distributing the inter-core teleportation operations uniformly over the execution time-slices. The burstiness for the VQE HEA_2 instance of 60 cores displays a higher burstiness since a high number of CNOT gates are required to be executed in parallel. We record a substantial increase in the teleportation instructions as a direct result of distributing the program over more cores. The QFT instance showcases a high number of teleportations due its particular all-to-one two-qubit interactions. The QAOA_02 circuit also indicates a high number of teleportations owing to the high-density and scattered pattern of the applied operations. The surging number of teleportations in these two circuits translates to a low average qubit staytime, which is related to the qubit movements necessary to comply with the communication requirements. This means qubits are moved

around extensively to ensure proximate qubit placement, hence a restrictive communication overhead. The qubits in the other circuits are generally stationary since the two-qubit gates are mostly applied on adjacent qubits in case of sequential gates, or between qubits placed in the same core. This analysis would estimate the computational and communication resources required for the algorithm execution on large-scale modular architectures, which is useful for optimizing compilation techniques such as optimal initial placement and state routing.

4.3 Weak scaling

It is noteworthy that all circuits were executed at the size of 512 qubits, except for the QAOA_02 and QFT circuits which were implemented for 256 qubits due to high computational costs and current limitations of the compiler.

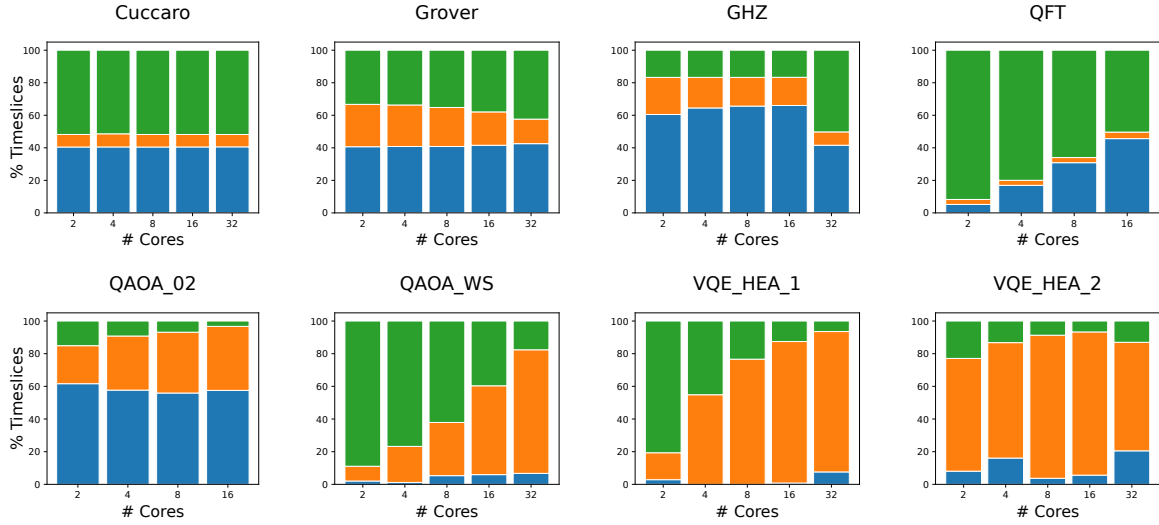


Fig. 6. Distribution of computation and communication operations over the execution timeslices in the weak scaling. Blue, orange, and green indicate the communication, parallel communication and computation, and computation operations, respectively.

The distribution of computation and communication operations over the execution time is depicted in Figure 6. This indicates that the system achieves optimal task parallelization rate for the Cuccaro and Grover circuits for all core sizes. These circuits display local, short-range sequential two-qubit gates. Therefore, the amount of inter-core teleportation instructions required is low. Generally, we note an increasing amount of inter-core communications as we add more cores, such as displayed intelligibly for the QFT circuit. The system achieves a high task parallelization rate particularly for the QAOA_WS and the VQE circuits. As the GHZ circuit structure requires long-range cross-core operations, the substantial surge in inter-core communication is prohibiting the computational operations. The compiler improves the instruction distribution when the number of cores is large. A similar behaviour is observed in the QAOA_02 circuit. The low inter-core communication requirements for circuits of a small number of cores is explained by the high number of qubits placed in each core.

We consider the performance metrics to assess the capacity of the system capacity in executing the given algorithms in the weak scaling as presented in Figure 7. The computation-to-communication rate approaches

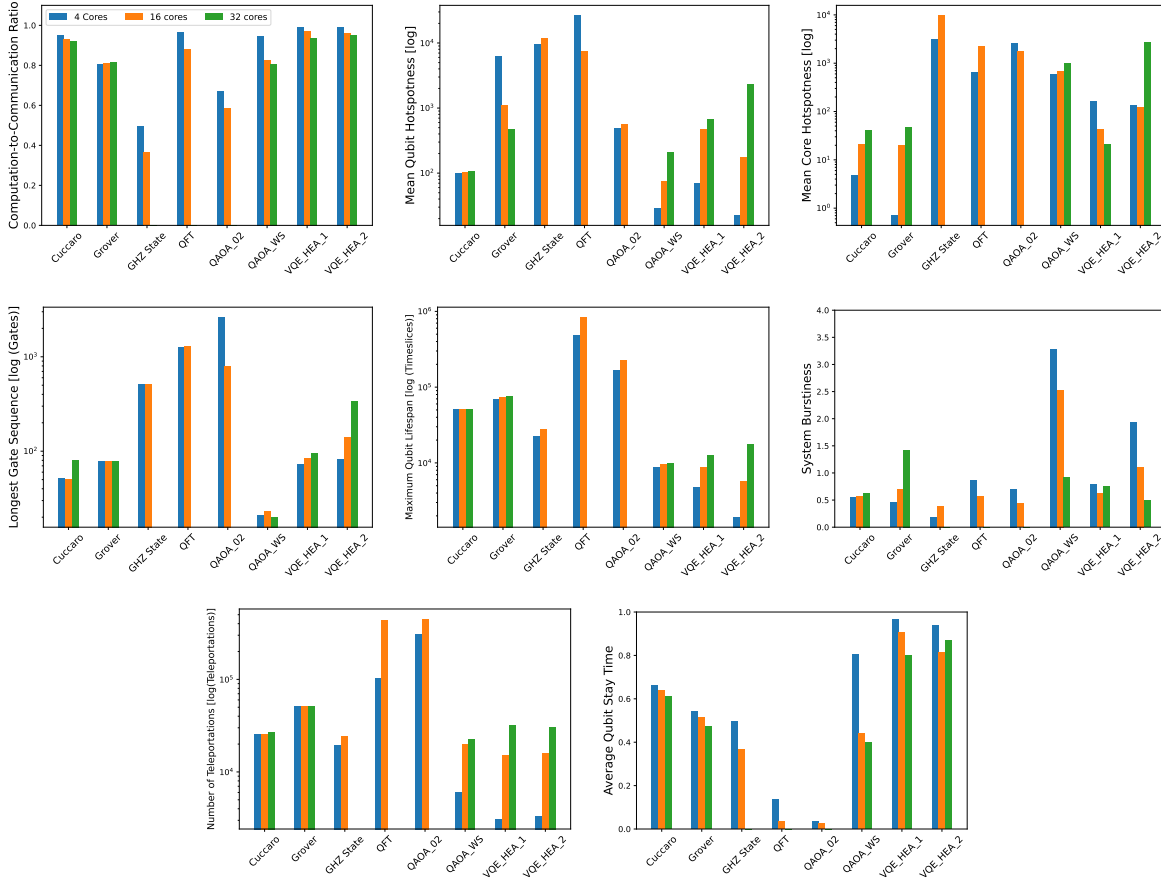


Fig. 7. Performance metrics for the selected algorithms executed on large-scale modular architectures supporting around 1000 qubits in the weak scaling

1 for circuits across varying architecture sizes, with the GHZ State showcasing the lowest ratio, indicating the computational resources outweigh the communication resources. The mean qubit hotspottness typically depends on the distribution of operations of each circuit at each size as part of the compilation process. We note a prominent qubit hotspottness decrease in the QFT circuit as we scale the architecture, as opposed to the GHZ instance, despite both circuit structures showcasing extensive cross-core two-qubit instructions. The mean core hotspottness tends to increase as we scale the number of cores for all types of circuits. The longest gate sequence and the qubit lifespan continuously increase since more communication operations are implemented, especially for circuits with a high density of cross-core two-qubit gates, mainly QFT. The graph-dependent, random operation distribution in the QAOA_02 circuit gives an explanation for the decrease in the longest gate sequence applied as we scale the architecture. We denote a relatively low communication burstiness for all circuits, although it is decidedly determined by the circuit specific structure. The number of teleportations in all circuits substantially increases as a consequence of distributing the programs over additional cores, with the amount of instructions required remains particularly high for the QFT and QAOA_02 instances. This directly

justifies the corresponding low qubit stay-time in comparison with the remaining circuits. The average qubit stay time is considerably high in the weak scaling since the cores host a large number of qubits and therefore the inter-core state exchange requirements is limited.

5 DISCUSSION

In this paper, we investigate the inter-core qubit traffic on a modular quantum system of increasing sizes in the strong scaling and weak scaling. We therefore evaluate the performance of the system in executing various quantum algorithms within the constraints imposed by inter-core communication. Specifically, we focus on the impact of inter-core communication on the computational process, considering a specific mapping algorithm, an all-to-all qubit connectivity, and assuming the teleportation protocol for inter-core state transfer. By analyzing the circuit mapping to physical qubits, we can observe the distribution of communication qubits and computation qubits during the program execution. The circuit mapping process efficiency is dependent on both the algorithm structure and the underlying architecture. The algorithm structure determines the number of gates, the two-qubit interactions and the inter-core communication requirements. Adding more cores results in a substantial increase in inter-core teleportation operations to comply with the computational tasks, imposing a higher communication overhead. Therefore, it would be pertinent to investigate the adequate trade-off of the number of qubit per core and the total number of cores relatively to the circuit size and structure. On a general note, to optimize circuit mapping, it is recommended to employ a compilation technique that minimizes qubit movements across cores by defining the optimal qubit initial placement considering the underlying architecture, and allocating the necessary communication and computation qubits on the processor. Communication qubits should be allocated without penalizing the necessary computation resources, which can be achieved by utilizing the idling qubits in the execution process as communication qubits, provided their quantum states are not used for computation.

In the strong scaling, we note that increasing the size of the problem typically amplifies the inter-core communication overhead. More inter-core communications lead to a higher likelihood of qubit movements across cores, resulting in a decreased computational efficiency in terms of runtime. Algorithms that involve short-range two-qubit gates applied sequentially on local or adjacent qubits demonstrate a better performance in parallelizing communication and computation tasks, as well as efficiently applying the necessary communication tasks without delaying the computation process. On the other hand, circuits with a high number of two-qubit gates applied across chips, even if applied sequentially, indicate a growing amount of inter-core communications that hinder the computation process. Circuits with a high density of parallel two-qubit gates demonstrate a comparable behaviour.

In the weak scaling, circuits exhibiting short-range, local two-qubit gates applied on adjacent qubits achieve a high parallelization rate of computation and communication tasks. As the number of cores increases, the inter-core communication overhead is expected to grow for circuits with a high density of parallel two-qubit operations. It is noteworthy that the communication overhead on the computation process is less prevalent in the weak scaling since the number of qubits per core is higher, and therefore less inter-core state exchanges are required.

Our analysis provides a qualitative understanding of workload characteristics when executing various quantum algorithms on large-scale modular architectures. We indicate that the computational and communication resources required for the program execution in the strong scaling and weak scaling are typically similar, and can be predicted for compiler optimization purposes based on the results we presented. Incorporating parameters such as the estimated duration of teleportation operations across cores, realistic processor topologies, and the state transfer process fidelity would enable a quantitative assessment of the impact of communication overhead on the computational process. This informative analysis would assist hardware designers in determining the optimal number of qubits per core to build robust modular architectures, and network designers in identifying

ideal communication channel parameters that minimize state transfer fidelity losses and latencies. Additionally, the presented results suggest that designing algorithms employing short-range, local two-qubit gates applied on adjacent qubits, or qubits placed within the same processor, is better adapted to the execution on modular architectures. While inter-core communication are the key feature of modular processors, reducing the communication overhead is crucial for a high-fidelity computational process.

6 CONCLUSIONS AND OUTLOOK

Designing efficient inter-core communications is the key feature of building modular quantum computers to scale the current processors. As the technology is developing, we present a qualitative characterization of the inter-core qubit traffic in modular quantum processors supporting around 1000 qubits, representing the computation and inter-core communication workloads in large-scale architectures.

In this work, we demonstrate that circuit mapping is a crucial step in the compilation process that considers essentially the circuit structure and the underlying architecture. Optimizing circuit mapping algorithms for modular architectures entails defining an optimal qubit initial placement and allocating the necessary communication and computation qubits on the processor, in addition to designing circuit-compatible processor topologies. Additionally, we propose a set of performance metrics to assess the communication overhead and computation resources necessary to execute quantum application algorithms on large-scale modular processors. This estimates the program execution efficiency of the system within the constraints of communications networks. While the necessary computational and communication resources highly depend on the input circuit's structure, we show that all the executed quantum circuits are parallelizable with significant resources allocated to the computational tasks, the resource usage tends to increase as we scale the circuit size, the temporal locality increases proportionally to the number of cores, and the spatial locality increases respectively to the number of qubits per core.

Our work contributes to setting the foundations of benchmarking modular quantum processors by proposing performance metrics and an application-oriented characterization of modular quantum computers. In future works, we evaluate the performance of the system considering the circuit interaction graph and the topology of quantum processors, aiming for a comprehensive assessment of modular quantum architectures.

ACKNOWLEDGMENTS

Authors gratefully acknowledge funding from the European Commission through HORIZON-EIC-2022-PATHFINDEROPEN-01-101099697 (QUADRATURE) and grant HORIZON-ERC-2021-101042080 (WINC).

REFERENCES

- [1] Sergi Abadal, Raúl Martínez, Josep Solé-Pareta, Eduard Alarcón, and Albert Cabellos-Aparicio. 2016. Characterization and modeling of multicast communication in cache-coherent manycore processors. *Computers & Electrical Engineering* 51 (2016), 168–183. <https://doi.org/10.1016/j.compeleceng.2015.12.018>
- [2] Sergi Abadal, Albert Mestres, Raúl Martínez, Eduard Alarcón, Albert Cabellos-Aparicio, and Raul Martinez. 2015. Multicast On-chip Traffic Analysis Targeting Manycore NoC Design. In *2015 23rd Euromicro International Conference on Parallel, Distributed, and Network-Based Processing*. 370–378. <https://doi.org/10.1109/PDP.2015.26>
- [3] Google Quantum AI. 2022. Cirq: An open source framework for programming quantum computers. <https://quantumai.google/cirq>
- [4] Thomas Alexander, Naoki Kanazawa, Daniel J Egger, Lauren Capelluto, Christopher J Wood, Ali Javadi-Abhari, and David C McKay. 2020. Qiskit pulse: programming quantum computers through the cloud with pulses. *Quantum Science and Technology* 5, 4 (aug 2020), 044006. <https://doi.org/10.1088/2058-9565/aba404>
- [5] Jonathan M. Baker, Casey Duckering, Alexander Hoover, and Frederic T. Chong. 2020. Time-sliced quantum circuit partitioning for modular architectures. In *Proceedings of the 17th ACM International Conference on Computing Frontiers*. ACM. <https://doi.org/10.1145/3387902.3392617>
- [6] Medina Bandic, Luise Prielinger, Jonas Nüßlein, Anabel Ovide, Santiago Rodrigo, Sergi Abadal, Hans van Someren, Gayane Vardoyan, Eduard Alarcon, Carmen G. Almudever, and Sebastian Feld. 2023. Mapping quantum circuits to modular architectures with QUBO.

- <https://doi.org/10.48550/arXiv.2305.06687>
- [7] Medina Bandić, Carmen G. Almudever, and Sebastian Feld. 2022. Interaction graph-based profiling of quantum benchmarks for improving quantum circuit mapping techniques. arXiv:2212.06640 [quant-ph]
 - [8] Nick Barrow-Williams, Christian Fensch, and Simon Moore. 2009. A communication characterisation of Splash-2 and Parsec. In *2009 IEEE International Symposium on Workload Characterization (IISWC)*. 86–97. <https://doi.org/10.1109/IISWC.2009.5306792>
 - [9] Kishor Bharti, Alba Cervera-Lierta, Thi Ha Kyaw, Tobias Haug, Sumner Alperin-Lea, Abhinav Anand, Matthias Degroote, Hermanni Heimonen, Jakob S. Kottmann, Tim Menke, Wai-Keong Mok, Sukin Sim, Leong-Chuan Kwek, and Alán Aspuru-Guzik. 2022. Noisy intermediate-scale quantum algorithms. *Reviews of Modern Physics* 94, 1 (feb 2022). <https://doi.org/10.1103/revmodphys.94.015004>
 - [10] Jacob Biamonte, Peter Witte, Nicola Pancotti, Patrick Rebentrost, Nathan Wiebe, and Seth Lloyd. 2017. Quantum machine learning. *Nature* 549, 7671 (13 Sept. 2017), 195–202. <https://doi.org/10.1038/nature23474>
 - [11] Paul Bogdan and Radu Marculescu. 2011. Non-Stationary Traffic Analysis and Its Implications on Multicore Platform Design. *IEEE Transactions on Computer-Aided Design of Integrated Circuits and Systems* 30, 4 (2011), 508–519. <https://doi.org/10.1109/TCAD.2011.2111270>
 - [12] Sergey Bravyi, Oliver Dial, Jay M. Gambetta, Darío Gil, and Zaira Nazario. 2022. The future of quantum computing with superconducting qubits. *Journal of Applied Physics* 132, 16 (10 2022). <https://doi.org/10.1063/5.0082975>
 - [13] Kenneth R. Brown, Jungsang Kim, and Christopher Monroe. 2016. Co-designing a scalable quantum computer with trapped atomic ions. *npj Quantum Information* 2 (2016). <https://api.semanticscholar.org/CorpusID:28267210>
 - [14] Andrew W. Cross, Lev S. Bishop, Sarah Sheldon, Paul D. Nation, and Jay M. Gambetta. 2019. Validating quantum computers using randomized model circuits. *Phys. Rev. A* 100 (Sep 2019), 032328. Issue 3. <https://doi.org/10.1103/PhysRevA.100.032328>
 - [15] Steven Cuccaro, Thomas Draper, Samuel Kutin, and David Moulton. 2004. A new quantum ripple-carry addition circuit. (11 2004).
 - [16] David Culler, Jaswinder Pal Singh, and Anoop Gupta. 1998. *Parallel Computer Architecture: A Hardware/Software Approach*. Morgan Kaufmann Publishers Inc., San Francisco, CA, USA.
 - [17] Yulong Dong and Lin Lin. 2021. Random circuit block-encoded matrix and a proposal of quantum LINPACK benchmark. *Physical Review A* 103, 6 (jun 2021). <https://doi.org/10.1103/physreva.103.062412>
 - [18] Yuxuan Du, Min-Hsiu Hsieh, Tongliang Liu, and Dacheng Tao. 2021. A Grover-search Based Quantum Learning Scheme for Classification. *New Journal of Physics* 23 (02 2021). <https://doi.org/10.1088/1367-2630/abdefa>
 - [19] P Erdős and A Rényi. 1959. On Random Graphs I. *Publicationes Mathematicae Debrecen* 6 (1959), 290–297.
 - [20] Pau Escofet, Anable Ovide, Carmen G. Almudever, Eduard Alarcón, and Sergi Abadal. 2023. Hungarian Qubit Assignment for Optimized Mapping of Quantum Circuits on Multi-Core Architectures. *IEEE Computer Architecture Letters* (2023). <https://doi.org/10.1109/LCA.2023.3318857> arXiv:<https://arxiv.org/abs/2309.12182>
 - [21] Pau Escofet et al. 2023. Interconnect Fabrics for Multi-Core Quantum Processors: A Context Analysis. (2023). <https://doi.org/10.48550/arXiv.2309.07313> arXiv:<https://arxiv.org/abs/2309.07313>
 - [22] Edward Farhi, Jeffrey Goldstone, and Sam Gutmann. 2014. A Quantum Approximate Optimization Algorithm. arXiv:1411.4028 [quant-ph]
 - [23] Davide Ferrari, Angela Sara Cacciapuoti, Michele Amoretti, and Marcello Caleffi. 2021. Compiler Design for Distributed Quantum Computing. *IEEE Transactions on Quantum Engineering* 2 (2021), 1–20. <https://doi.org/10.1109/TQE.2021.3053921>
 - [24] Alysson Gold, JP Paquette, Anna Stockklauser, Matthew J. Reagor, M. Sohaib Alam, Andrew Bestwick, Nicolas Didier, Ani Nersisyan, Feyza Oruc, Armin Razavi, Ben Scharmann, Eyob A. Sete, Biswajit Sur, Davide Venturelli, Cody James Winkleblack, Filip Wudarski, Mike Harburn, and Chad Rigetti. 2021. Entanglement Across Separate Silicon Dies in a Modular Superconducting Qubit Device. <https://doi.org/10.1038/s41534-021-00484-1>
 - [25] Paul V. Gratz and Stephen W. Keckler. 2009. Realistic Workload Characterization and Analysis for Networks-on-Chip Design. <https://api.semanticscholar.org/CorpusID:12992323>
 - [26] Daniel M. Greenberger, Michael A. Horne, and Anton Zeilinger. 2007. Going Beyond Bell’s Theorem. arXiv:0712.0921 [quant-ph]
 - [27] Lov K. Grover. 1996. A fast quantum mechanical algorithm for database search. arXiv:quant-ph/9605043 [quant-ph]
 - [28] Divya P Gulati, Changkyu Kim, Simha Sethumadhavan, Stephen W Keckler, and Doug Burger. 2008. Multitasking workload scheduling on flexible-core chip multiprocessors. In *Proceedings of the 17th international conference on Parallel architectures and compilation techniques*. 187–196.
 - [29] Mohammad Reza Habibi, Saeed Golestan, Ali Soltanmanesh, Josep M. Guerrero, and Juan C. Vasquez. 2022. Power and Energy Applications Based on Quantum Computing: The Possible Potentials of Grover’s Algorithm. *Electronics* 11, 18 (2022). <https://doi.org/10.3390/electronics11182919>
 - [30] Hamza Jnane, Brennan Undseth, Zhenyu Cai, Simon C. Benjamin, and Bálint Koczor. 2022. Multicore Quantum Computing. *Phys. Rev. Appl.* 18 (Oct 2022), 044064. Issue 4. <https://doi.org/10.1103/PhysRevApplied.18.044064>
 - [31] V. Kaushal, B. Lekitsch, A. Stahl, J. Hilder, D. Pijn, C. Schmiegelow, A. Bermudez, M. Müller, F. Schmidt-Kaler, and U. Poschinger. 2020. Shuttling-based trapped-ion quantum information processing. *AVS Quantum Science* 2, 1 (03 2020). <https://doi.org/10.1116/1.5126186> 014101.

- [32] N. Khammassi, I. Ashraf, J. V. Someren, R. Nane, A. M. Krol, M. A. Rol, L. Lao, K. Bertels, and C. G. Almudever. 2021. OpenQL: A Portable Quantum Programming Framework for Quantum Accelerators. *J. Emerg. Technol. Comput. Syst.* 18, 1, Article 13 (dec 2021), 24 pages. <https://doi.org/10.1145/3474222>
- [33] E. Knill, D. Leibfried, R. Reichle, J. Britton, R. B. Blakestad, J. D. Jost, C. Langer, R. Ozeri, S. Seidelin, and D. J. Wineland. 2008. Randomized benchmarking of quantum gates. *Physical Review A* 77, 1 (jan 2008). <https://doi.org/10.1103/physreva.77.012307>
- [34] Masaaki Kondo, Hiroshi Sasaki, and Hiroshi Nakamura. 2007. Improving Fairness, Throughput and Energy-Efficiency on a Chip Multiprocessor through DVFS. *SIGARCH Comput. Archit. News* 35, 1 (mar 2007), 31–38. <https://doi.org/10.1145/1241601.1241609>
- [35] Ang Li, Samuel Stein, Sriram Krishnamoorthy, and James Ang. 2022. QASMBench: A Low-level QASM Benchmark Suite for NISQ Evaluation and Simulation. arXiv:2005.13018 [quant-ph]
- [36] Guang Hao Low and Isaac L. Chuang. 2019. Hamiltonian Simulation by Qubitization. *Quantum* 3 (jul 2019), 163. <https://doi.org/10.22331/q-2019-07-12-163>
- [37] Brian Marinelli, Jie Luo, Hengjiang Ren, Bethany M. Niedzielski, David K. Kim, Rabindra Das, Mollie Schwartz, David I. Santiago, and Irfan Siddiqi. 2023. Dynamically Reconfigurable Photon Exchange in a Superconducting Quantum Processor. (3 2023). arXiv:2303.03507 [quant-ph]
- [38] Koen Mesman, Zaid Al-Ars, and Matthias Möller. 2022. QPack: Quantum Approximate Optimization Algorithms as universal benchmark for quantum computers. arXiv:2103.17193 [cs.ET]
- [39] Microsoft. [n. d.]. Microsoft/QSHARP-language: Official Repository for design of the quantum programming language Q# and its core libraries. <https://github.com/microsoft/qsharp-language>
- [40] Michael A. Nielsen and Isaac L. Chuang. 2010. *Quantum Computation and Quantum Information: 10th Anniversary Edition*. Cambridge University Press. <https://doi.org/10.1017/CBO9780511976667>
- [41] Michael A. Nielsen and Isaac L. Chuang. 2011. *Quantum Computation and Quantum Information: 10th Anniversary Edition* (10th ed.). Cambridge University Press, USA.
- [42] Alexandru Paler and Simon J. Devitt. 2015. An introduction to Fault-tolerant Quantum Computing. arXiv:1508.03695 [quant-ph]
- [43] Alberto Peruzzo, Jarrod McClean, Peter Shadbolt, Man-Hong Yung, Xiao-Qi Zhou, Peter J. Love, Alán Aspuru-Guzik, and Jeremy L. O’Brien. 2014. A variational eigenvalue solver on a photonic quantum processor. *Nature Communications* 5, 1 (jul 2014). <https://doi.org/10.1038/ncomms5213>
- [44] John Preskill. 2018. Quantum Computing in the NISQ era and beyond. *Quantum* 2 (Aug. 2018), 79. <https://doi.org/10.22331/q-2018-08-06-79>
- [45] Santiago Rodrigo, Sergi Abadal, Eduard Alarcón, and Carmen G. Almudever. 2020. Will Quantum Computers Scale Without Inter-Chip Comms? A Structured Design Exploration to the Monolithic vs Distributed Architectures Quest. In *2020 XXXV Conference on Design of Circuits and Integrated Systems (DCIS)*. 1–6. <https://doi.org/10.1109/DCIS51330.2020.9268630>
- [46] Santiago Rodrigo, Sergi Abadal, Eduard Alarcón, Medina Bandic, Hans van Someren, and Carmen G. Almudéver. 2021. On Double Full-Stack Communication-Enabled Architectures for Multicore Quantum Computers. *IEEE Micro* 41, 5 (2021), 48–56. <https://doi.org/10.1109/MM.2021.3092706>
- [47] Santiago Rodrigo, Sergi Abadal, Carmen G. Almudéver, and Eduard Alarcón. 2021. Modelling Short-Range Quantum Teleportation for Scalable Multi-Core Quantum Computing Architectures. In *Proceedings of the Eight Annual ACM International Conference on Nanoscale Computing and Communication* (Virtual Event, Italy) (NANOCOM ’21). Association for Computing Machinery, New York, NY, USA, Article 14, 7 pages. <https://doi.org/10.1145/3477206.3477461>
- [48] Santiago Rodrigo, Domenico Spanò, Medina Bandic, Sergi Abadal, Hans van Someren, Anabel Ovide, Sebastian Feld, Carmen G. Almudéver, and Eduard Alarcón. 2022. Characterizing the Spatio-Temporal Qubit Traffic of a Quantum Intranet Aiming at Modular Quantum Computer Architectures. In *Proceedings of the 9th ACM International Conference on Nanoscale Computing and Communication* (Barcelona, Catalunya, Spain) (NANOCOM ’22). Association for Computing Machinery, New York, NY, USA, Article 8, 7 pages. <https://doi.org/10.1145/3558583.3558846>
- [49] Rodrigo Santiago, Sergi Abadal, Carmen Almudéver, and Eduard Alarcón. 2021. Modelling Short-range Quantum Teleportation for Scalable Multi-Core Quantum Computing Architectures. 1–7. <https://doi.org/10.1145/3477206.3477461>
- [50] Peter W. Shor. 1997. Polynomial-Time Algorithms for Prime Factorization and Discrete Logarithms on a Quantum Computer. *SIAM J. Comput.* 26, 5 (oct 1997), 1484–1509. <https://doi.org/10.1137/s0097539795293172>
- [51] V. Soteriou, Hangsheng Wang, and L. Peh. 2006. A Statistical Traffic Model for On-Chip Interconnection Networks. In *14th IEEE International Symposium on Modeling, Analysis, and Simulation*. 104–116. <https://doi.org/10.1109/MASCOTS.2006.9>
- [52] IonQ Staff. 2023. Algorithmic qubits: A better single-number metric. <https://ionq.com/resources/algorithmic-qubits-a-better-single-number-metric>
- [53] Wei Tang, Teague Tomesh, Martin Suchara, Jeffrey Larson, and Margaret Martonosi. 2021. CutQC: Using Small Quantum Computers for Large Quantum Circuit Evaluations. In *Proceedings of the 26th ACM International Conference on Architectural Support for Programming Languages and Operating Systems* (Virtual, USA) (ASPLOS ’21). Association for Computing Machinery, New York, NY, USA, 473–486. <https://doi.org/10.1145/3445814.3446758>

- [54] Jules Tilly, Hongxiang Chen, Shuxiang Cao, Dario Picozzi, Kanav Setia, Ying Li, Edward Grant, Leonard Wossnig, Ivan Rungger, George H. Booth, and Jonathan Tennyson. 2022. The Variational Quantum Eigensolver: A review of methods and best practices. *Physics Reports* 986 (nov 2022), 1–128. <https://doi.org/10.1016/j.physrep.2022.08.003>
- [55] Teague Tomesh, Pranav Gokhale, Victory Omole, Gokul Ravi, Kaitlin Smith, Joshua Vizslai, Xin-Chuan Wu, Nikos Hardavellas, Margaret Martonosi, and Frederic Chong. 2022. SupermarQ: A Scalable Quantum Benchmark Suite. 587–603. <https://doi.org/10.1109/HPCA53966.2022.00050>
- [56] Andrew Wack, Hanhee Paik, Ali Javadi-Abhari, Petar Jurcevic, Ismael Faro, Jay M. Gambetta, and Blake R. Johnson. 2021. Quality, Speed, and Scale: three key attributes to measure the performance of near-term quantum computers. arXiv:2110.14108 [quant-ph]
- [57] Duncan J. Watts and Steven H. Strogatz. 1998. Collective dynamics of ‘small-world’ networks. *Nature* 393, 6684 (1998), 440–442. <https://doi.org/10.1038/30918>
- [58] Stefan Woerner and Daniel J. Egger. 2019. Quantum risk analysis. *npj Quantum Information* 5, 1 (feb 2019). <https://doi.org/10.1038/s41534-019-0130-6>
- [59] William K Wootters and Wojciech H Zurek. 1982. A single quantum cannot be cloned. *Nature* (1982). <https://doi.org/10.1038/299802a0>
- [60] Chao Zhou, Pinlei Lu, Matthieu Praquin, Tzu Chiao Chien, Ryan Kaufman, Xi Cao, Mingkan Xia, Roger S.K. Mong, Wolfgang Pfaff, David Pekker, and Michael Hatridge. 2023. Realizing all-to-all couplings among detachable quantum modules using a microwave quantum state router. *npj Quantum Information* 9, 1 (Dec. 2023). <https://doi.org/10.1038/s41534-023-00723-7>

A ESTIMATED GATE COUNT

- (1) **The ripple-carry Cuccaro adder:** The gate count for this circuit depends on the number of qubits N representing the binary numbers being added. The gate count can be approximated as the number of Hadamard gates for state preparation $\approx O(N)$, and the two-qubit gates applied on the $N - 1$ carry qubits estimated as $\approx O(N)$. Therefore, the total gate count is $\approx O(N)$.
- (2) **The Grover’s search main routine:** The number of iterations, denoted k , applied to find the target element with a high probability is proportional to the total number of elements in the database. The gate count in a single iteration can be approximated as the number of single-qubit gates (Hadamard and X) used for state preparation $\approx O(N)$, the number of single-qubit gates $\approx O(N)$ and two-qubit gates applied to pairs of qubits $\approx O(N)$ in the oracle operator, the number of single-qubit gates $\approx O(N)$ and two-qubit gates applied to pairs of qubits $\approx O(N)$ in the diffuser operator. The total gate count can then be approximated as $\approx O(k \times N)$.
- (3) **The GHZ State circuit:** The gate count in this circuit is estimated as the Hadamard gate applied to the first qubit and the CNOT gates applied to $N - 1$ qubits. The total gate count is then estimated as $\approx O(N)$.
- (4) **The QFT circuit:** The gate count in this circuit is estimated as the number of Hadamard gates applied to each qubit $= O(N)$, and the number of Controlled-Phase gates $\approx O((N - 1) \times (N - q)) \approx O(N^2)$, and the number of SWAP operations applied to pairs of qubits $\approx O(N)$. The total gate count is then approximated as $\approx O(N^2)$.
- (5) **The QAOA MaxCut ansatz circuit:** The number of ansatz layers, denoted l , is a tunable parameter. The gate count in a single layer is approximated as the number of Hadamard gates required for state preparation $\approx O(N)$, the number of single-qubit z-rotation gates $\approx O(N)$ and two-qubit gates applied to pairs of qubits $\approx O(N)$ in the Problem Hamiltonian operator, and the number of single-qubit x-rotation gates $\approx O(N)$ applied in the Mixer Hamiltonian operator to all qubits. The total gate count is then estimated as $\approx O(l \times N)$.
- (6) **The VQE Hardware Efficient ansatz circuit:** The number of ansatz layers, denoted l , is a tunable parameter. The gate count in a single layer is approximated as the number of single-qubit x-rotation and y-rotation $\approx O(N)$ applied to qubits, and the number of CNOT gates applied to pairs of qubits $\approx O(N)$. The total gate count is then estimated as $\approx O(l \times N)$.

B CIRCUIT MAPPING TRACES

We hereby present the circuit traces for virtual and physical mapping of the various selected algorithms in Figure 8 and Figure 9, respectively. We observe the initial circuit structure in virtual circuit mappings: the Grover’s circuit showcasing the iterative oracle-diffuser cycle, the GHZ State circuit exhibiting a sequential CNOT gate ladder applied from the first qubit to all the qubits, the QFT instance illustrating the SWAP-ed pattern of a single qubit interaction with all the remaining ones, the random operations in the QAOA_02 circuit imposed by the random Erdos Renyi input graph as opposed to the short-ranged and highly clustered operations determined by the Watts Strogatz input graph in the QAOA_WS circuit. The two VQE ansatze implemented demonstrate distinct traces as imposed by order of CNOT gate application. The execution traces of circuit mapping to physical qubits indicate the structural changes made during the compilation process to comply with the underlying modular architecture and inter-core communication requirements.

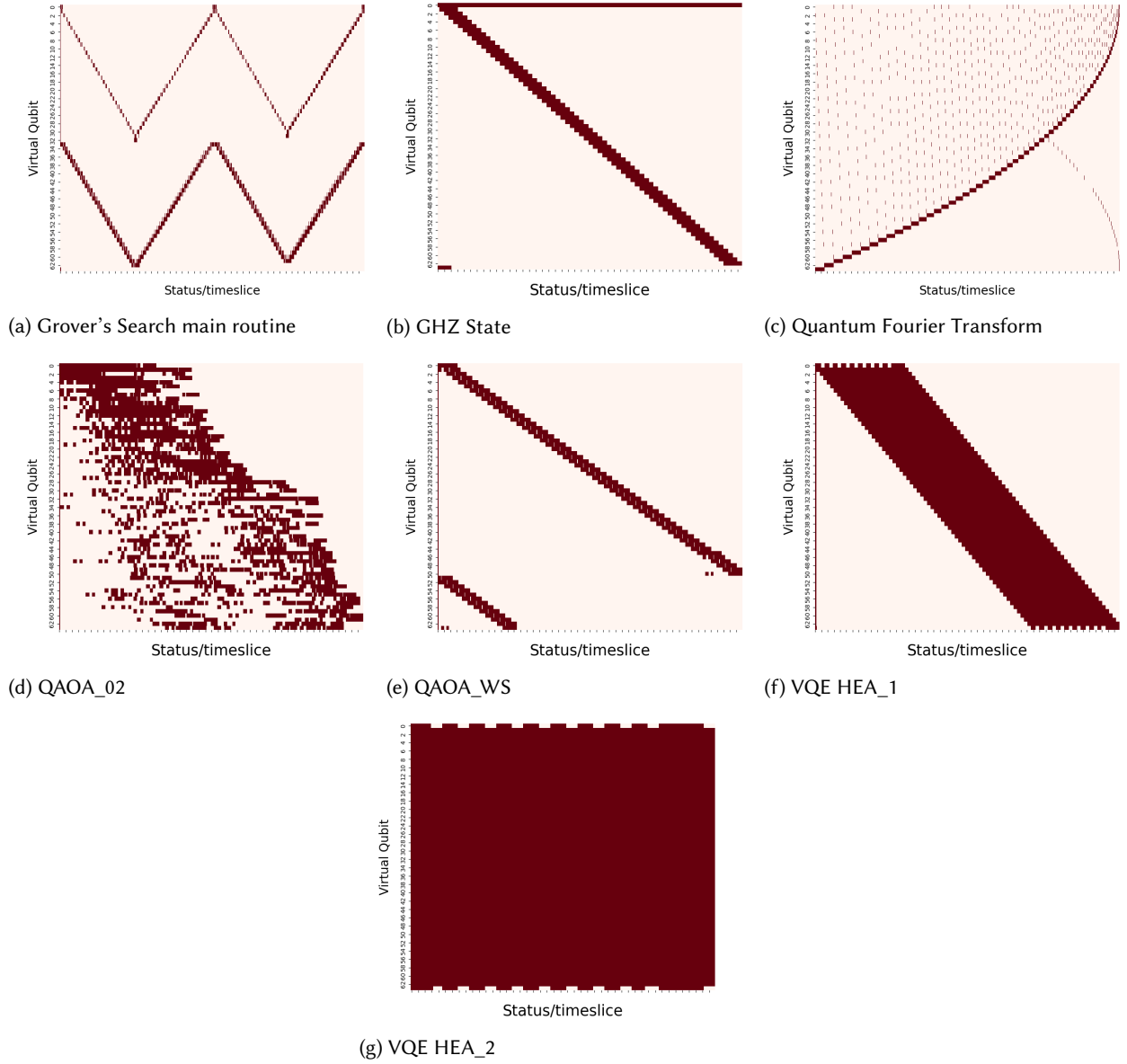


Fig. 8. Circuit mapping traces to virtual qubits on an architecture of 64 qubits . Computation times are represented in red.

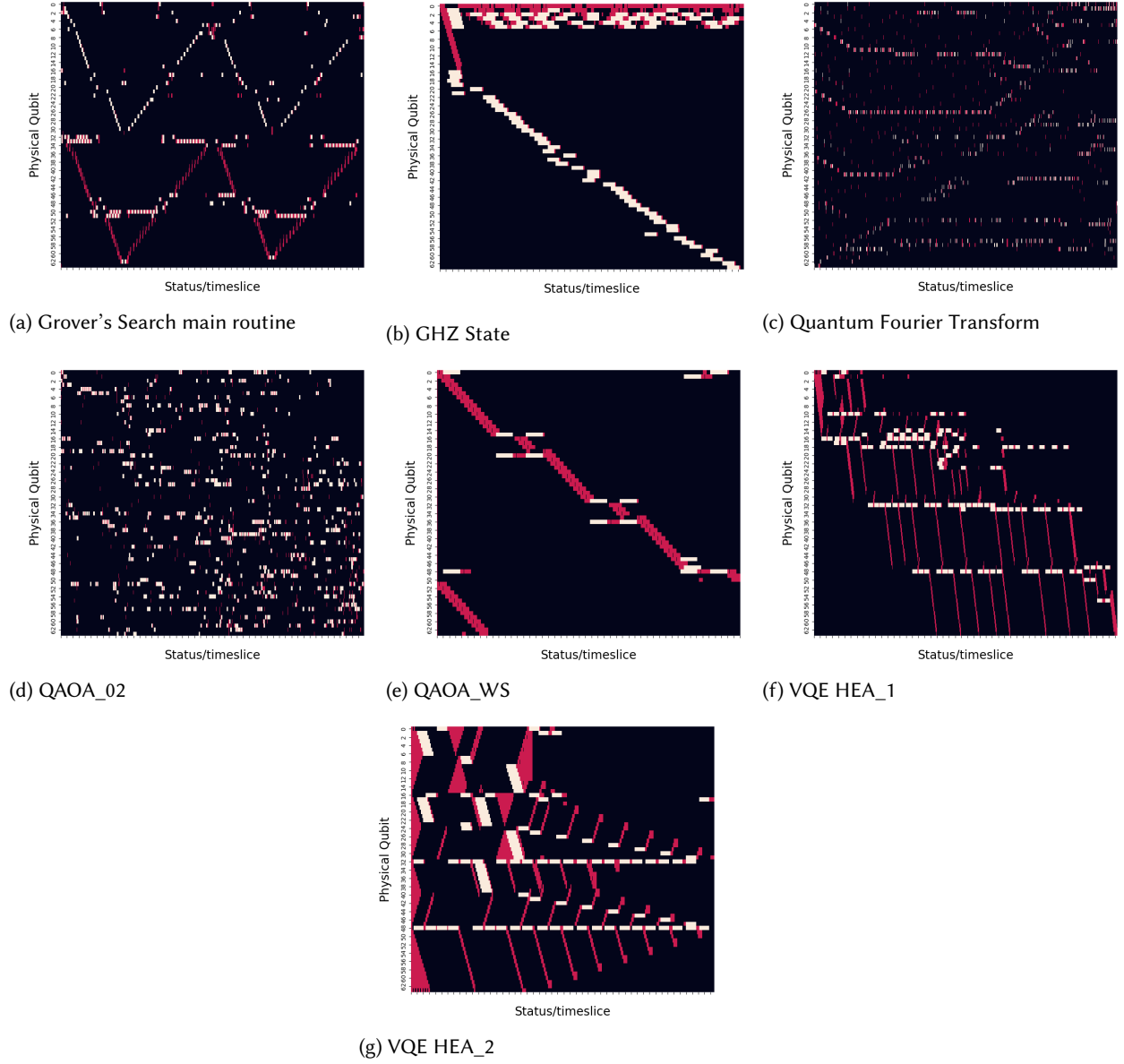


Fig. 9. Circuit mapping traces to physical qubits on a modular architecture of 16 qubits \times 4 cores with all-to-all connectivity. Computation, communication, and idling times are represented in red, white, and black, respectively